TOPICAL REVIEW — High pressure physics

High pressure structural phase transitions of TiO_2 nanomaterials*

Quan-Jun Li(李全军) and Bing-Bing Liu(刘冰冰)†

State Key Laboratory of Superhard Materials, Jilin University, Changchun 130012, *China*

(Received 5 June 2015; revised manuscript received 2 July 2015; published online 9 June 2016)

Recently, the high pressure study on the TiO_2 nanomaterials has attracted considerable attention due to the typical crystal structure and the fascinating properties of TiO_2 with nanoscale sizes. In this paper, we briefly review the recent progress in the high pressure phase transitions of TiO_2 nanomaterials. We discuss the size effects and morphology effects on the high pressure phase transitions of TiO_2 nanomaterials with different particle sizes, morphologies, and microstructures. Several typical pressure-induced structural phase transitions in TiO_2 nanomaterials are presented, including size-dependent phase transition selectivity in nanoparticles, morphology-tuned phase transition in nanowires, nanosheets, and nanoporous materials, and pressure-induced amorphization (PIA) and polyamorphism in ultrafine nanoparticles and TiO_2-B nanoribbons. Various TiO_2 nanostructural materials with high pressure structures are prepared successfully by high pressure treatment of the corresponding crystal nanomaterials, such as amorphous TiO_2 nanoribbons, α-PbO_2-type TiO_2 nanowires, nanosheets, and nanoporous materials. These studies suggest that the high pressure phase transitions of TiO_2 nanomaterials depend on the nanosize, morphology, interface energy, and microstructure. The diversity of high pressure behaviors of TiO_2 nanomaterials provides a new insight into the properties of nanomaterials, and paves a way for preparing new nanomaterials with novel high pressure structures and properties for various applications.

Keywords: high pressure, nanomaterials, phase transition, TiO_2

PACS: 61.46.Df **DOI:** 10.1088/1674-1056/25/7/076107

1. Introduction

As an important semiconductor, TiO_2 has been extensively studied because of its wide applications in photocatalysis, gas sensors, energy storage, biotechnology, etc.[1–5] There are four polymorphs of TiO_2 in nature: anatase (tetragonal $I4_1/amd$), rutile (tetragonal $P4/mnm$), brookite (orthorhombic $Pbca$), and TiO_2-B (monoclinic $C2/m$). Among these polymorphs, anatase and rutile are the most common types of TiO_2 and have been widely studied because of their representative structures. It is well known that the anatase transforms first into an orthorhombic α-PbO_2 phase at the pressure range of 2–5 GPa, and then to a baddeleyite structure (monoclinic $P2_1/c$) at higher pressure ($>$ 10 GPa).[6,7] The rutile phase converts into the baddeleyite form at $\sim$ 12 GPa.[8] The phase transition from the baddeleyite to the α-PbO_2 is observed in both anatase and rutile samples upon decompression.[6–8] In addition, the cotunnite structure TiO_2 (orthorhombic $Pnma$) was synthesized at pressure above 60 GPa and temperatures above 1000 K, which is considered as the least compressible and hardest oxide.[9] The fluorite TiO_2 ($Fm3m$) was prepared at 48 GPa by heating anatase to 1900–2100 K and was proved to be a possible ultrahard material by theoretical calculation.[10] These previous studies indicate that there are abundant high pressure structures in TiO_2.

In recent years, TiO_2 nanomaterials received considerable interest because of their improved physical and chemical properties due to the small size or large surface area. The increased surface-area-to-volume ratio when the particle size reaches the nanoscale results in new physical properties, including unusual pressure responses, especially for TiO_2. The previous studies on high pressure phase transitions of TiO_2 nanomaterials have revealed a series of interesting phenomena. For instance, the enhanced phase transition pressure with a decrease in particle size was observed in most of TiO_2 nanoparticles.[11–17] Direct transition to the baddeleyite phase occurred in the anatase nanoparticles with size of 12–50 nm, nanowires, and nanosheets, which shows that an energy barrier exists in the anatase-to-α-PbO_2 transition for the nanoparticles.[11,15,18–20] The pressure-induced amorphization (PIA) and polyamorphism were found in the ultrafine anatase nanoparticles ($<$ 12 nm) and TiO_2-B nanoribbons.[15,21] The polyamorphism was explained by the structural relationship with the corresponding high pressure phases. These results indicated that the size can influence both the phase transition pressure and the phase transition sequence. For the rutile TiO_2 nanoparticles, the decreased transition pressure of rutile-to-baddeleyite was found in Wang's report,[22] while the opposite results were given in Gerward's study.[23] There are still some controversies in the high pressure phase transition behaviors of rutile TiO_2,[22–27] which is probably related to the particle size, stoichiometry, surface and interface conditions, and hy-

*Project supported by the National Basic Research Program of China (Grant No. 2011CB808200), the National Natural Science Foundation of China (Grant Nos. 11374120, 11004075, 10979001, 51025206, 51032001, and 21073071), and the Cheung Kong Scholars Programme of China.

†Corresponding author. E-mail: liubb@jlu.edu.cn

© 2016 Chinese Physical Society and IOP Publishing Ltd

drostaticity. More recently, morphology-tuned high pressure phase transitions have been found in TiO_2 nanomaterials with various morphologies or shapes.[17–21] Shape-dependent compressibility was found in rice-shaped and rod-shaped anatase nanoparticles, and ultralow compressibility was found in the rod-shaped nanoparticles.[17] The morphology-tuned phase transition sequence in the anatase nanowires[18,19] indicated that morphology can also significantly influence the high pressure behavior as well as nanosize.

High pressure study on nanomaterials has attracted more and more attention in the last decade. As a typical nanomaterial, TiO_2 nanomaterials show unique phase transition behaviors under high pressure. In this paper, we will briefly review the recent progress in the high pressure study of TiO_2 nanomaterials. In Section 2, we review the work in size-effects on the high pressure phase transitions, in which the size-dependent phase transition selectivity in nanoparticles with different sizes is discussed. In Section 3, we present the PIA and polyamorphism in ultrafine anatase TiO_2 nanoparticles, nanoporous material, and TiO_2-B nanoribbons. In Section 4, we review the work in morphology effects on the high pressure behaviors, including morphology-tuned phase transitions in nanowires and nanoporous material, and enhanced bulk moduli in rice-shaped nanoparticles and nanosheets with highly reactive {001} facets. Finally, we give a concluding remark in Section 5.

2. Size effects on the high pressure phase transitions

It is well known that nanomaterials have extraordinary physical and chemical properties resulting from the nanosize effect. TiO_2 nanomaterials show extensive new physical and chemical properties compared with their bulk. High pressure can modify the atomic distance, atomic interaction, atomic arrangement, and crystal structure, which provides an effective way to study the new phenomena and properties of the nanomaterials. Recently, high pressure study on the nanomaterials has attracted great enthusiasm because of the strong size effects on the phase transition.[28–30] TiO_2 has been widely studied as one of the typical models for the high pressure study of size effect. In the following, we will discuss the recent progress in the size effects on the high pressure phase transition of TiO_2 nanoparticles without specific morphology or shape.

Swamy *et al.*[31] observed the direct transition from anatase to baddeleyite in TiO_2 nanoparticles with a crystallite size of 30–40 nm. Later, Hearne *et al.*[12] further found the anatase–baddeleyite transition in TiO_2 nanoparticles ($\sim$ 12 nm). They pointed out that the formation of baddeleyite is more favorable than that of α-PbO_2 because of the lower-energy grain boundaries of the small size anatase nanoparticles. There is a minimum or critical diameter for the nuclei of the α-PbO_2 phase in TiO_2 nanoparticles, which is estimated to be $\sim$ 15 nm. This indicates that the α-PbO_2 phase will only appear when the particle size is smaller than the critical diameter. In addition, the estimated critical diameter for the baddeleyite phase is $\sim$ 4 nm. When the TiO_2 nanoparticle is in the size range of 4–12 nm, the anatase–baddeleyite transition is energetically favored. Although these critical diameters are estimated, experimental evidence is still needed. Consequently, more detailed experimental study about the size effects was reported in Swamy's work.[11] They revealed the unique size-dependent phase selectivity of anatase under high pressure. As shown in Fig. 1, we can see three size regimes: (i) the common anatase-α-PbO_2 transition occurs above 2 GPa and then the baddeleyite phase forms at 12–15 GPa in TiO_2 macrocrystals ($>$ 50 nm); (ii) the anatase phase transforms into baddeleyite structure directly at 12–20 GPa in TiO_2 nanoparticles with middle size (12–50 nm); (iii) amorphization takes place above 18 GPa in ultrafine TiO_2 nanoparticles ($<$ 10 nm).

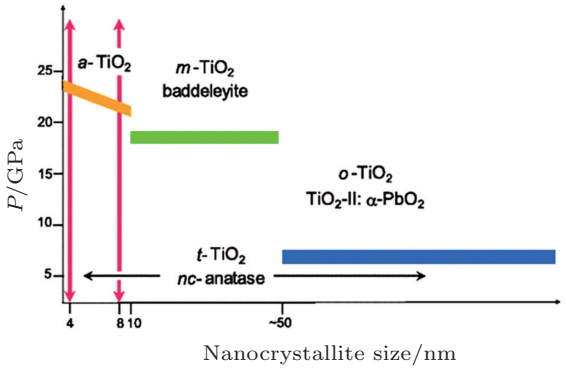


Fig. 1. (color online) Size-dependent pressure stability of TiO_2 nanoparticles. The average transition pressures of the three phase transition regimes are shown. Nanocrystals of size $<$ 10 nm undergo PIA and remain amorphous (a-TiO_2) upon further compression and decompression. Approximately 12–50 nm crystallites transform to m-TiO_2 upon compression, which then transform to o-TiO_2 on decompression. Coarser crystallites transform directly to o-TiO_2. Reprinted with permission from Ref. [15], Copyright (2006) by the American Physical Society.

Besides the phase transition sequence, the compressibility of TiO_2 nanoparticles also can be influenced by the nanosize effects. Numbers of previous studies have demonstrated that the nanocrystalline material is less compressible than the corresponding bulk, that is, the TiO_2 nanoparticles show an enhanced bulk modulus compared with the macrocrystalline TiO_2.[14,15,22,31] However, a different view also exists in various groups. Al-Khatatbeh *et al.*[32] reported the size dependence of the bulk modulus for anatase TiO_2 nanoparticles under hydrostatic conditions. Figure 2 shows the change in the bulk modulus of anatase TiO_2 nanoparticles with the grain size. The constant bulk modulus ($\sim$ 200 GPa) is found in anatase TiO_2 with a grain size larger than 40 nm. There is a $\sim$ 15% decrease in bulk modulus for $\sim$ 20 nm grains, suggesting a rapid increase in compressibility for anatase TiO_2

nanoparticles with size of 20–40 nm, while the bulk modulus of anatase shows no size-dependent in the grain size range from 6 nm to 20 nm.

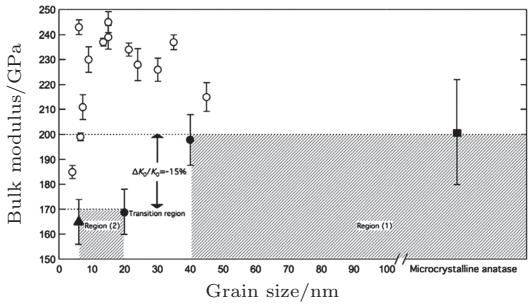


Fig. 2. The change in bulk modulus of anatase as a function of grain size. Closed symbols show Al-Khatatbeh's results[32] (circles) and those of the microcrystalline TiO_2 anatase (square) and 6 nm nc-nc-TiO_2 nantase (triangle). The bulk modulus of anatase is size-independent in at least two regions: from microcrystalline size down to 40 nm and from 6 nm to 20 nm. The region between 20 nm and 40 nm indicates a transition region for nc-TiO_2 anatase. Reprinted with permission from Ref. [32], Copyright (2012) by the American Chemical Society.

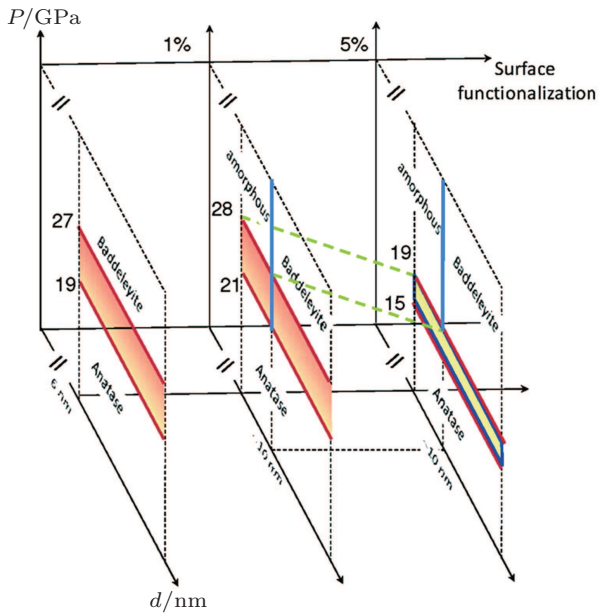


Fig. 3. (color online) Phase diagram including size, pressure, and surface functionalization as control parameters. In the absence of functionalization, the anatase structure in nanoparticles will transform to the baddeleyite phase (at least for $d > 6$ nm). In the case of surface functionalization, the defects' density will orientate the transformation to an amorphous state for $d < 10$ nm. Reprinted with permission from Ref. [36], Copyright (2011) by the American Chemical Society.

The surface energy shows a significant impact on the phase transition of the TiO_2 nanoparticles besides nanosize. Machon *et al.*[33] investigated the interface energy effect on the high pressure phase transition of TiO_2 nanoparticles with size of 6 nm. As shown in Fig. 3, the pressure-induced amorphization takes place in the TiO_2 nanoparticles with citrate molecules at the surface, while the anatase–baddeleyite transition occurs in the bare TiO_2 nanoparticles. The crystal-to-crystal transition is obviously different from that of the PIA in ultrafine TiO_2 nanoparticles.[14,15] The small amount of citrate molecules at the particle surface plays important roles in the phase transition of anatase nanoparticles. The size effect is not sufficient for inducing amorphization. They pointed out that the results relating to PIA driven by the size effect should be re-examined. The chemical effect needs to be considered together with the size effect. There still exist some controversies that require further experimental and theoretical studies.

3. Pressure-induced amorphization

PIA is an important subject in earth and planetary sciences, physics, chemistry, and material science. This phenomenon was observed in ice (H_2O),[34] Si,[35] SiO_2,[36] and other tetrahedrally coordinated solids generally. Recently, size-dependent amorphization was found in some octahedrally coordinated nanomaterials, such as Y_2O_3,[37] Gd_2O_3,[38] and TiO_2.[14–16,21,39,40] In particular, the unique polyamorphism was observed in the TiO_2 nanomaterials for the first time, that is a transition between a high density amorphous (HDA) and a low density amorphous (LDA), which is similar to that of ice and Si.[35,41–43] The PIA and polyamorphism have attracted much attention in the last decade. In the following, several size-dependent amorphization and polyamorphism in anatase TiO_2 nanoparticles are discussed. Besides, we present our recent work on the PIA and polyamorphization in TiO_2-B nanoribbons.

Several groups have observed the PIA in TiO_2 nanoparticles with ultrafine size below ~12 nm.[14–16] In those studies, the starting anatase phase transforms into the HDA form directly without passing through the high pressure phases of α-PbO_2 or baddeleyite, in which the surface energy plays important roles in the phase transition. Subsequently, Swamy *et al.*[15] reported the HDA–LDA polyamorphism, which demonstrated that the HDA TiO_2 formed by PIA at high pressure transforms into an LDA-TiO_2 polyamorph during decompression (Fig. 4). This study suggests that the HDA and LDA forms have a relationship to the α-PbO_2 and baddeleyite structures according to the XRD and Raman results, respectively. Pischedda *et al.*[14] found that ultrafine ~ 6 nm grain-size nanoanatase retains its structural integrity up to 18 GPa, and transforms into a highly disordered state at higher pressures. They suggested that disorder initiates in the surface shell of the nanograin by molecular dynamics simulations. The ultrastability of the ultrafine nanoanatase may be explained in terms of nucleation and growth criteria. The crystalline size is comparable to or smaller than a critical diameter, and thus the emergence of the high pressure phases (baddeleyite, α-PbO_2, or any other) is not energetically favorable. Therefore, PIA occurs in these ultrafine anatase nanoparticles. Flank *et al.*[16] have further investigated the PIA and polyamorphism transition in nanosized TiO_2 by using x-ray absorption spectroscopy.

They found the difference between the HDA and LDA forms. In the HDA state, the Ti atom is surrounded by 3 ± 0.5 oxygen at 1.89 Å and 3 ± 0.5 oxygen at 2.07 Å, while in the LDA state, Ti is surrounded by 2 ± 0.5 oxygen at 1.84 Å and 2 ± 0.5 oxygen at 2.06 Å; they are very different from each other. In addition, a precursor-ordered structural phase was observed before amorphization in this study. Machon *et al.*[40] revealed different polyamorphisms in the mechanically prepared amorphous TiO_2 nanoparticles and the chemically prepared amorphous TiO_2 nanoparticles. A new high density amorphous state (HDA2) was observed at around 21 GPa in the chemically prepared amorphous nanoparticles, which further transforms into HDA1 state at $\sim$ 30 GPa (Fig. 5). This indicates that the high pressure polyamorphic transformations significantly depend on the starting amorphous material. Those studies have made progress in exploring PIA and polyamorphism. However, the nature of the transition between the HDA and LDA still remains unclear.

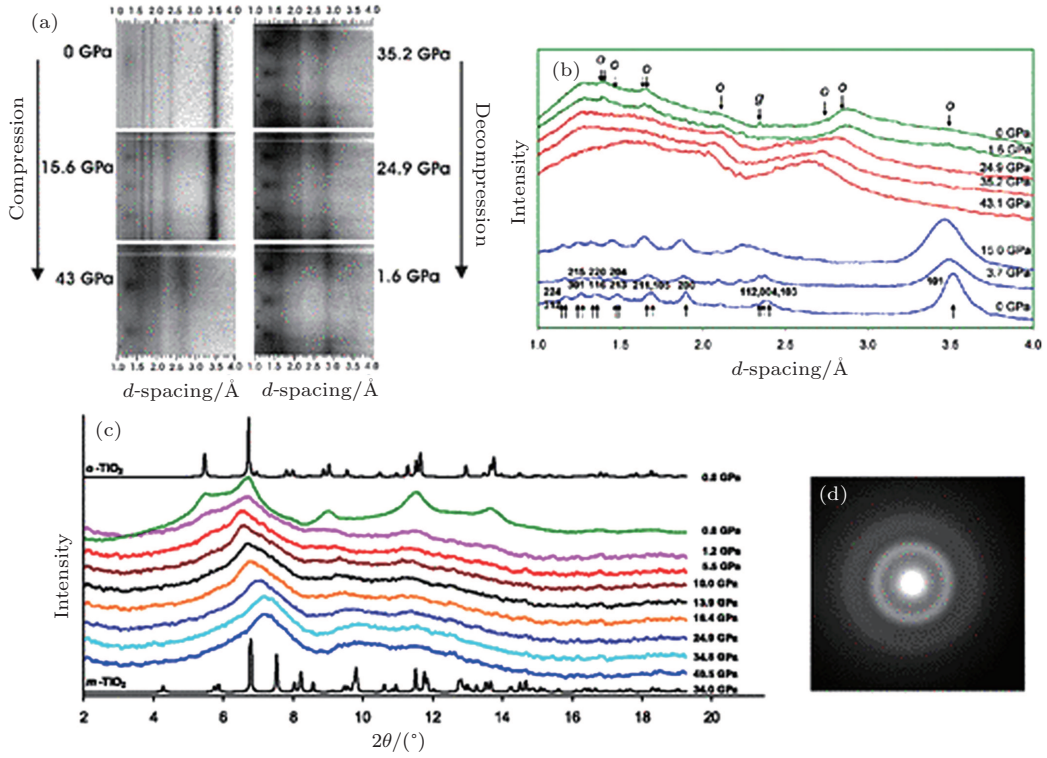


Fig. 4. (color online) Synchrotron XRD data obtained during compression and decompression of TiO_2 nanoparticles. (a) PIA takes place in 8 nm particles at $\sim$ 20 GPa (left column). The amorphous phase is recovered under ambient conditions, but subtle changes in the XRD pattern, including increased ordering at low pressures, are observed upon decompression (right column). (b) Integrated XRD data of 8 nm particles during compression or decompression runs. Anatase (t-TiO_2) reflections are indicated by up arrows; arrows labeled "o" and "g" represent o-TiO_2 and Au diffraction positions at 0 GPa. (c) Integrated XRD data of 4 nm particles obtained during decompression. Calculated XRD spectra (for wavelength $\lambda = 0.3344$ Å) of o-TiO_2 and m-TiO_2 are given for comparison. The 0 GPa (outside the DAC) spectrum of pressure-amorphized 8 nm particles exhibits diffuse scattering background characteristic of a highly disordered material, with perhaps structural similarity to o-TiO_2. (d) Electron diffraction, however, confirms the amorphous nature of the material at a length scale of that of a crystalline unit cell ($\sim$ 1 nm). Reprinted with permission from Ref. [5], Copyright (2006) by the American Physical Society.

Recently, we further investigated the PIA and polyamorphism in one-dimensional single-crystal TiO_2-B nanoribbons.[21] TiO_2-B is a metastable TiO_2 polymorph with monoclinic structure (space group $C2/m$) composed of corrugated sheets of edge- and corner-sharing TiO_6 octahedra. As shown in Fig. 6, TiO_2-B transforms into HDA form directly above 16 GPa upon compression. This is obviously different from that of the corresponding bulk, which converts into anatase phase at $\sim$ 6 GPa. Upon decompression, the HDA form transforms into an LDA form. The XRD results indicate that the HDA and LDA forms also show a relationship to the α-PbO_2 and baddeleyite structures, respectively. To further investigate the structural relationship, we performed HRTEM observation for the quenched sample. Figure 7 shows the HRTEM images of the LDA TiO_2 nanoribbons. Uniform nanoribbons with lengths of several micrometers and widths of 50–200 nm can be seen clearly, which indicates that the nanoribbons retain their pristine morphology. From Fig. 7(c), it is clear that a long-range ordered structure does not exist in the LDA nanoribbons, but some short-range ordered domains (1–3 nm) are distributed inside the nanoribbons. The spacing of the lattice fringes of these domains is 0.283 nm, which corresponds to the (111) plane of the α-PbO_2 phase. This result demonstrates that the structural relationship between the LDA form and the α-PbO_2 phase originates from these short-range domains. In this work, PIA and polyamorphism

were first observed in the one-dimensional TiO_2 nanomaterials. Moreover, the structural relationship between the LDA form and the α-PbO_2 phase was revealed directly for the first time by HRTEM. It also provides a new method for preparing one-dimensional amorphous nanomaterials from crystalline nanomaterials.

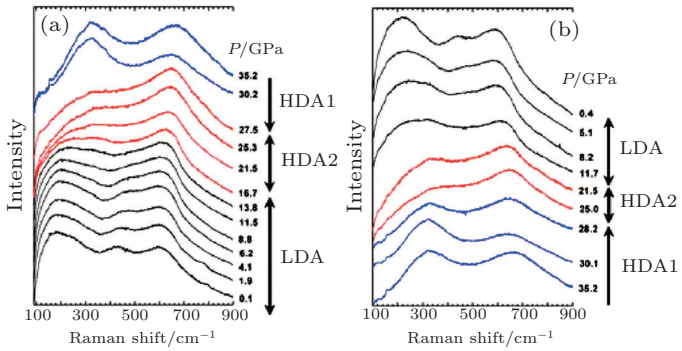


Fig. 5. (color online) (a) Raman spectra of 6 nm amorphous particles prepared by sol–gel synthesis with increasing pressure. An LDA to a new HDA2 transformation is observed above 16.7 GPa. Above 30.2 GPa, another amorphous state (HDA) appears. (b) Raman spectra of 6 nm amorphous particles with decreasing pressure. The back transformation HDA1–HDA2 is observed in the range of 28.2–25.0 GPa and the transformation HDA2–LDA starts around 11.7 GPa. Reprinted with permission from Ref. [40], Copyright (2010) by the American Physical Society.

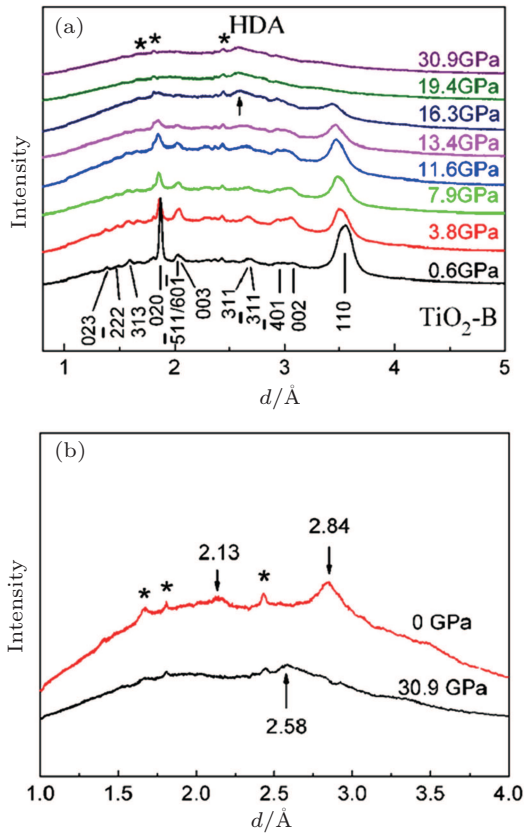


Fig. 6. (color online) (a) High pressure powder x-ray diffraction patterns of TiO_2-B nanoribbons up to 30.9 GPa at room temperature. (b) A comparison between the x-ray patterns of the as-synthesized TiO_2-B nanoribbons obtained at 30.9 GPa and recovered at ambient conditions. Three weak peaks (marked with asterisks) are derived from the energy-dispersive synchrotron x-ray diffraction system. The figure is reproduced from Ref. [21].

In addition, we found that nanoporous anatase TiO_2 transforms directly to the baddeleyite phase with poor crystallinity at pressure of 15–18 GPa, and amorphization occurs eventually at the pressure above 20 GPa (Fig. 8(a)).[44] The phase transition onset pressure of the anatase to the baddeleyite for the nanoporous anatase is lower than that of the corresponding anatase nanomaterials[11,12] and higher than that of the counterpart bulk.[8] Upon decompression, the amorphous form recovers to the baddeleyite structure at $\sim$ 12 GPa and then to the α-PbO_2 phase at $\sim$ 3.9 GPa (Fig. 8(b)). The reversible transition of the baddeleyite to the amorphous form occurs in the nanoporous anatase in which the poor crystalline baddeleyite phase acts as an intermediate state during the compression–decompression cycle. This is different from the PIA and polyamorphism in the anatase nanoparticles.[11,15] These results show that the porous microstructure may induce high stress at the contact points between grains of nanoparticles, and results in lattice distortion and even disorder finally. Obviously, the nanoporous structure may contribute to the high pressure phase transitions of the nanoporous anatase.

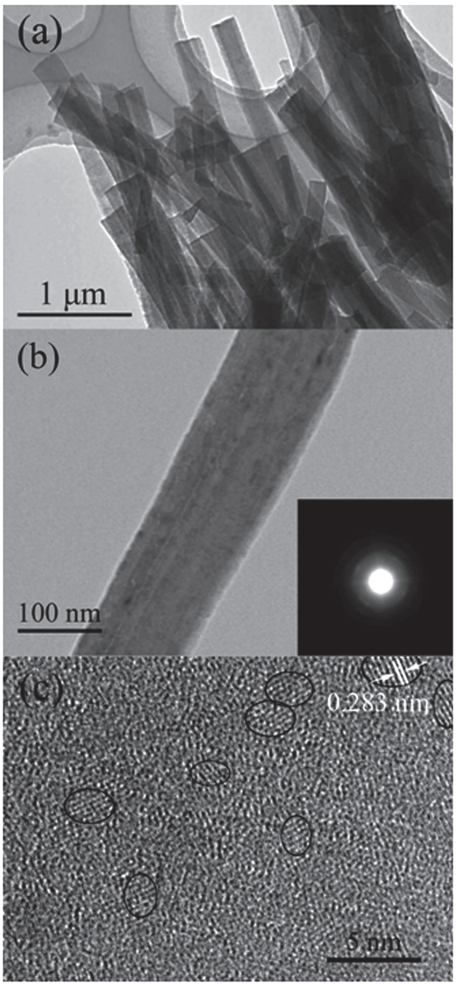


Fig. 7. TEM image of the nanoribbons after they were released from 31 GPa to ambient pressure. (a) Typical TEM image of LDA TiO_2 nanoribbons, (b) an individual LDA TiO_2 nanoribbon and its SAED (inset image), (c) HRTEM image of an individual LDA TiO_2 nanoribbon. The figure is reproduced from Ref. [21].

More recently, we prepared amorphous TiO_2 nanotubes with diameters of 8–10 nm and lengths of several nanometers by high pressure treatment of anatase TiO_2 nanotubes. PIA and polyamorphism were observed in this case, which is in good agreement with the previous results in ultrafine TiO_2 nanoparticles. We suggested that the unique open-ended nanotube morphology permits the pressure-transmitting media (4:1 methanol–ethanol mixture) to penetrate into the channels of nanotubes which may be of benefit to retain their tubular morphology. The small diameter and wall thickness of the TiO_2 nanotubes preclude the emergence of the high pressure phases and thus lead to the amorphization under high pressure. These results indicate that both the morphology and size play important roles in the PIA and polyamorphism of TiO_2 nanotubes. It also provides a new route for preparing amorphous nanomaterials by high pressure treatment of corresponding crystal nanomaterials.

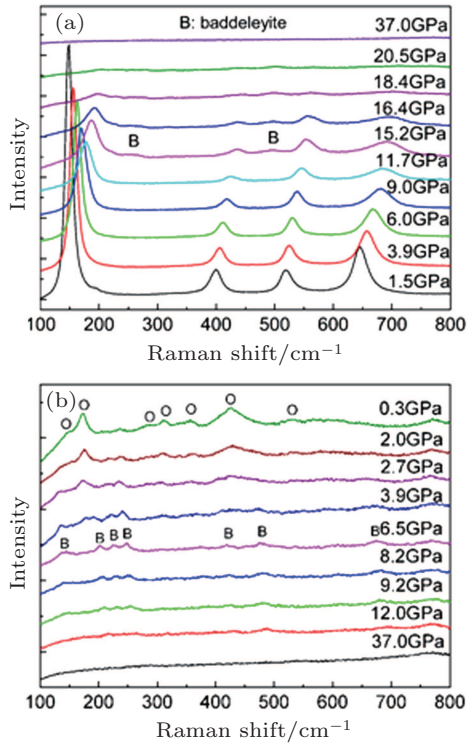


Fig. 8. (color online) Raman spectra of the nanoporous anatase TiO_2 at various pressures: (a) compression, (b) decompression. "B" and "O" denote the baddeleyite phase and the α-PbO_2 phase, respectively. The figure is reproduced from Ref. [44].

4. Morphology effects on the high pressure phase transitions

In general, the properties of nanomaterials strongly depend on their size and morphology. The size effects on the high pressure phase transition have been widely studied in TiO_2 nanomaterials. Recently, some studies also have indicated that the morphology shows vital effects on the phase transition pressure and sequence in nanomaterials.[45–49] The morphology-tuned phase transitions were found in nanostructural TiO_2 materials. Here, we will discuss the morphology effects on the high pressure behaviors of TiO_2 nanomaterials.

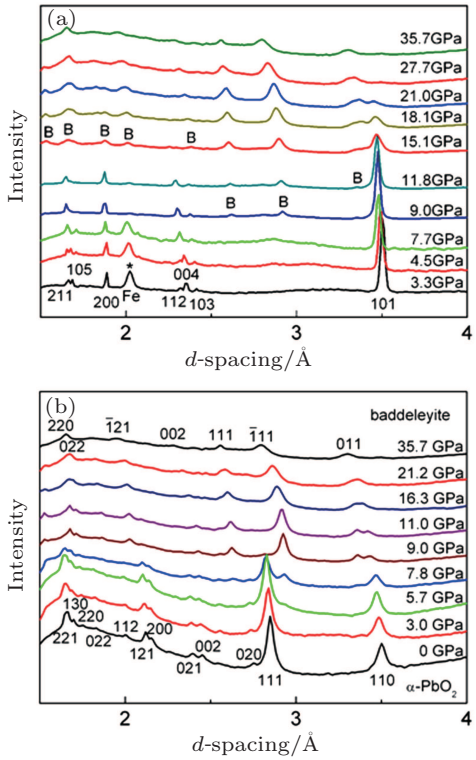


Fig. 9. (color online) XRD patterns of TiO_2 nanowires at selected pressures: (a) compression, (b) decompression. The diffraction peaks for baddeleyite phase are marked as B. The figure is reproduced from Ref. [18].

Park *et al.*[17] reported their study on shape-dependent compressibility of anatase TiO_2 nanoparticles. They found that the rice-shaped (3.8 nm×5.0 nm) nanoparticles show a reduced bulk modulus (204 (8) GPa), whereas the rod-shaped (3.5 nm×21.0 nm) nanoparticles exhibit an enhanced modulus (319 (20) GPa) compared to the counterpart bulk. It is clear that the morphology influences the bulk compressibility of TiO_2 nanoparticles. The largest bulk modulus of the rice-shaped nanoparticles in their study was interpreted by the enhanced spatial restrictions on size and shape control. After that, morphology-tuned phase transitions of anatase TiO_2 nanowires with diameter of 50–200 nm were studied by our group.[18] As shown in Fig. 9, the starting anatase phase starts to transform into baddeleyite phase at $\sim$ 9 GPa, and then the transition completes at above 21 GPa. This phase transition sequence is significantly different from that of the anatase nanoparticles with diameters larger than 50 nm, but is similar to that of the nanoparticles with diameters of 12–50 nm.[11,15] Upon decompression, the baddeleyite structure converts into α-PbO_2 phase. It is known that morphology and crystalline growth direction show important influences on the anisotropic compressibility of TiO_2 nanomaterials. Therefore,

a larger decrease rate of c/c_0 in the TiO_2 nanowires can be attributed to their nanowire-like morphology and crystal growth orientation. The bulk modulus (176 (9) GPa) of the TiO_2 nanowires is close to that of the bulk counterpart[13] but much smaller than that of most nanoparticles.[16,31] Figure 10 shows the TEM/HRTEM images for the quenched samples. It can be seen that the samples still retain their nanowire-like morphology (Fig. 10(a)). The two lattice spaces of ~ 0.28 nm and ~ 0.34 nm correspond to the (111) and (110) planes of the α-PbO_2 phase (Fig. 10(b)), respectively. This means that the quenched samples are α-PbO_2 phase TiO_2 nanowires. These results demonstrate that the nanoscale quasi-1D structure plays a dominant role in the high pressure transition.

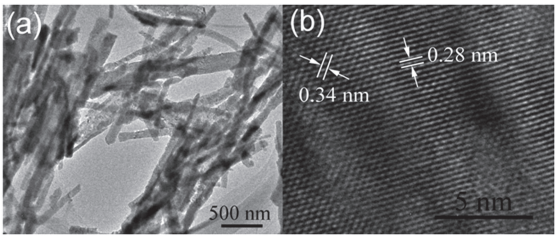


Fig. 10. (a) TEM and (b) HRTEM images of the TiO_2 nanowires after being released from ~ 35.7 GPa. The figure is reproduced from Ref. [18].

Dong *et al.*[19] further investigated the structural transformations of two hydrothermally synthesized TiO_2 nanowires with different diameters of < 100 nm and ~ 200 nm under high pressure up to 37 GPa. The direct anatase to baddeleyite phase transition was also found in both samples. However, the onset transition pressure for the small size nanowires (~ 13 GPa) is dramatically higher than that of the large size nanowires. The enhanced surface energy of the small size nanowires is the main reason for the elevated transition pressure compared to the large nanowires. Compared with the bulk TiO_2, the α-PbO_2 phase is bypassed in the anatase–baddeleyite transition of these TiO_2 nanowires. This is consistent with the phase transition sequence of those nanoparticles with diameters of 12–50 nm.[12,15] The enhanced surface energy for both sizes of TiO_2 nanowires hinders the formation of the α-PbO_2 phase which makes the baddeleyite structure become the more energetically favored structure under high pressure. These results further demonstrate that both the size and morphology influence the high pressure behaviors of TiO_2 nanowires.

Surface energy shows a significant contribution to high pressure phase transition in most nanomaterials, which leads to an increase of the phase transition pressure and modifies the phase transition sequence. However, we found that the high surface energy does not exhibit obvious effects on the high pressure behaviors of TiO_2 nanosheets with high reactive $\{001\}$ facets.[20] As shown in Fig. 11, the single-crystal anatase TiO_2 nanosheets are dominated by highly reactive $\{001\}$ facets. The thickness and the length of the nanosheets are 5–8 nm and 20–40 nm, respectively. The nanosheets have ultrafine thickness (5–8 nm) along the c axis of anatase TiO_2. Upon compression, the starting anatase phase transforms into baddeleyite structure directly at about 14.6 GPa (Fig. 12(a)). With further increasing pressure, the baddeleyite phase with poor crystalline forms and is stable up to the highest experimental pressure (35.8 GPa). The baddeleyite phase transforms into α-PbO_2 phase upon decompression (Fig. 12(b)). The phase transition behaviors are in good agreement with those of TiO_2 nanoparticles.[11,31] It is interesting that the c axis of the nanosheets is less compressible than that of TiO_2 bulk and nanoparticles. The obvious nanoconfinement of c-axis results in fewer soft empty O6 octahedral units in the nanosheets, which may be the main reason. Accordingly, the nanosheets show an ultrahigh bulk modulus (317 (10) GPa), which is much higher

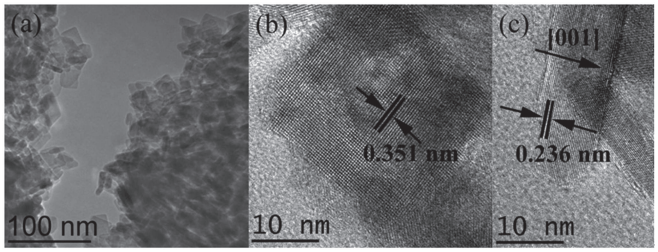


Fig. 11. (a) TEM and (b), (c) HRTEM images of TiO_2 nanosheets. The figure is reproduced from Ref. [20].

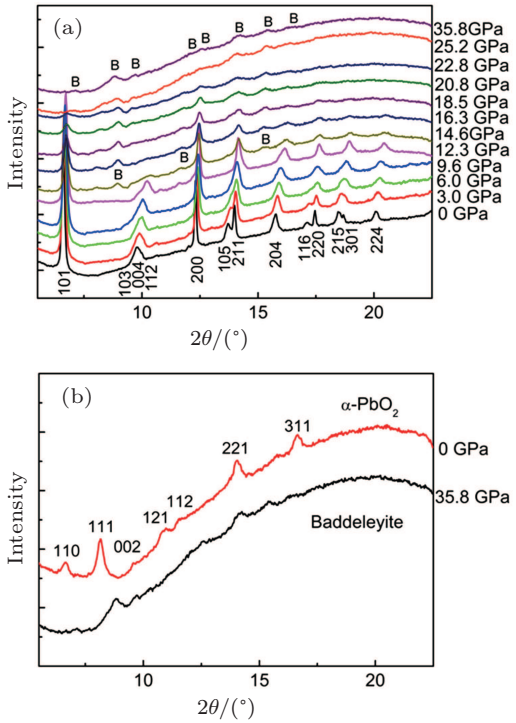


Fig. 12. Selected x-ray diffraction patterns of TiO_2 nanosheets under high pressures: (a) compression, (b) decompression. The diffraction peaks for baddeleyite phase are marked as B. The figure is reproduced from Ref. [20].

than that of bulk and nanoparticles but similar to that of the rice-shaped nanoparticles.[17] We suggest that the nanosheet enhanced bulk modulus can be attributed to their morphology with ultrafine thickness along the c axis. After quenching to ambient conditions, the nanosheets retain their pristine morphology but with the high pressure structure of α-PbO_2 phase. For the nanosheets with highly reactive $\{001\}$ facets, the surface energy is much higher than that of the other nanoparticles. According to the previous studies, the high surface energy would lead to an increase of the phase transition pressure in TiO_2 nanoparticles. However, the phase transition pressure is lower than that of the corresponding nanoparticles. These results indicate that the unique phase transition behaviors are dominated by the significant nanoconfinement effects along the c axis rather than the surface energy.

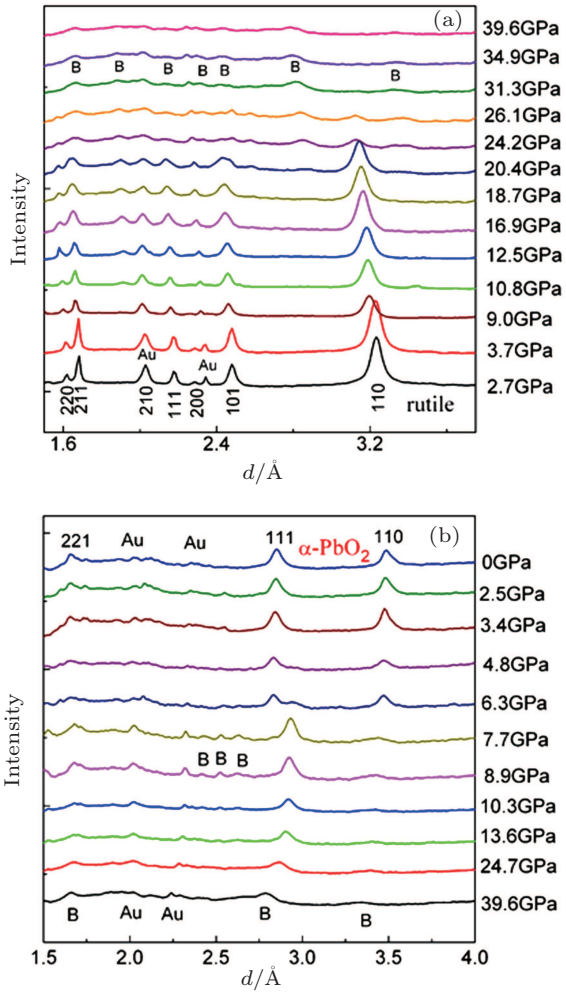


Fig. 13. High pressure powder x-ray diffraction patterns of nanoporous TiO_2: (a) compression, (b) decompression. Reflections marked B originate from baddeleyite-TiO_2. The figure is reproduced from Ref. [50].

Nanoporous TiO_2 has also attracted much attention because of their high surface area, porosity, and rich surface chemistry. We preformed the high pressure study for nanoporous rutile TiO_2.[50] As shown in Fig. 13, the rutile phase transforms into baddeleyite phase at 10.8 GPa, and the high pressure phase remains stable up to the highest pressure of 39.6 GPa. The obtained bulk modulus of the nanoporous rutile TiO_2 (204 (4) GPa) is lower than that of the corresponding bulk (230 (7) GPa) and nanoparticles (211 (7) GPa).[23,51] Upon decompression, the baddeleyite phase converts into α-PbO_2 phase. From Fig. 14, we can see that the quenched sample still retains the pristine nanoporous microstructure consisting of a number of $\sim$ 10 nm nanoparticles with the α-PbO_2 structure. These results show that the nanoporous rutile TiO_2 has excellent structural durability under high pressure. Upon compression, the nanoporous structure and the inside transmitting media assemble into a compound nanostructure which shows excellent tenacity. The enhanced fracture toughness can be attributed to the creep of the nanoparticles that is similar to the nanoceramics. Obviously, nanoporous microstructures can also modify the high pressure behaviors of TiO_2.

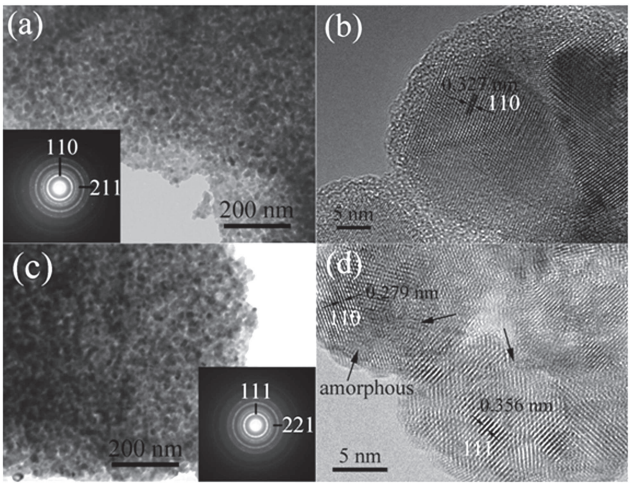


Fig. 14. (a) TEM and (b) HRTEM images of the pristine nanoporous TiO_2, (c) TEM and (d) HETEM images of the nanoporous TiO_2 after being released from 38.8 GPa. The arrows denote the distorted and disordered areas. The figure is reproduced from Ref. [50].

5. Conclusions and outlook

In the preceding sections, we have shown that the high pressure phase transitions of TiO_2 nanomaterials depend strongly on the size, morphology, microstructure, and interface energy. The increase of the transition pressure was found in TiO_2 nanoparticles with decreasing size. Unique size-dependent phase transition was revealed in TiO_2 nanoparticles with different size distribution ranges. Macrocrystals with size $>$ 50 nm show the routine transition sequence of anatase to α-PbO_2 to baddeleyite upon compression. In the size range of 12–50 nm, anatase nanoparticles transform into baddeleyite phase directly. For the smaller ($<$ 10 nm) nanoparticles, the anatase phase transforms into a HDA form without passing through any high pressure crystal phases upon compression, and the HDA converts into an LDA form upon decompression. We studied the PIA and polyamorphism in one-dimensional single-crystal TiO_2-B nanoribbons and revealed

the polyamorphism in terms of the structural relationships with high pressure crystal phases. The PIA and polyamorphism were first observed in the octahedrally coordinated TiO_2, providing a new window for investigation of amorphization in oxides. Shape-dependent compressibility was found in TiO_2 nanorice, nanorods, and nanosheets, in which the nanorice and nanosheets show ultrahigh bulk moduli compared with the other shaped nanoparticles and bulk. Morphology-tuned phase transition from anatase to baddeleyite was observed in TiO_2 nanowires with different sizes, which shows that the nanowire's morphology plays a critical role in the phase transition. In addition, the interface energy also exhibits a significant impact on the structural stability and phase transition of TiO_2 nanoparticles. A series of TiO_2 nanostructures with high pressure structures were obtained, such as amorphous TiO_2 nanoribbons, α-PbO_2-type TiO_2 nanowires, nanosheets, and nanoporous materials. These various high pressure phase transition behaviors of TiO_2 nanomaterials indicate that it is a very interesting topic in physics, chemistry, and material science. Although great progress has been made in this field, there is still a need to further explore the size and morphology effects on the phase transitions and properties of nanomaterials, especially for the rutile phase. It will be interesting to perform further study to understand the phase transition mechanism and explore the synthesis of TiO_2 nanomaterials with novel high pressure phases (e.g. ultrahard phase). This may bring new insight into the phase transition behaviors of nanomaterials under high pressure and provide a way for synthesizing novel functional nanomaterials with new structures.

References

[1] Yang H G, Sun C H, Qiao S Z, Zou J, Liu G, Smith S C, Cheng H M and Lu G Q 2008 *Nature* **453** 638
[2] Etgar L, Zhang W, Gabriel S, Hickey S G, Nazeeruddin M K, Eychmuller A, Liu B and Gratzel M 2012 *Adv. Mater.* **24** 2202
[3] Asahi R, Morikawa T, Ohwaki T, Aoki K and Taga Y 2001 *Science* **293** 269
[4] Chen X and Mao S S 2007 *Chem. Rev.* **107** 2891
[5] Chen X B, Liu L and Huang F Q 2015 *Chem. Rev.* **44** 1861
[6] Arlt T, Bermejo M, Blanco M A, Gerward L, Jiang J Z, Staun Olsen J, Recio J M and Recio J M 2000 *Phys. Rev. B* **61** 14414
[7] Lagarec K and Desgreniers S 1995 *Solid State Commun.* **94** 519
[8] Gerward L and Staun Olsen J 1997 *J. Appl. Cryst.* **30** 259
[9] Dubrovinsky L S, Dubrovinskaia N A, Swamy V. Muscat J, Harrison N M, Ahuja R, Holm B and Johansson B 2001 *Nature* **410** 653
[10] Swamy V and Muddle B C 2007 *Phys. Rev. Lett.* **98** 035502
[11] Swamy V, Kuznetsov A, Dubrovinsky L S, Caruso R A, Shchukin D G and Muddle B C 2005 *Phys. Rev. B* **71** 184302
[12] Hearne G R, Zhao J, Dawe A M, Pischedda V, Maaza M, Nieuwoudt M K, Kibasomba P, Nemraoui O, Comins J D and Witcomb M J 2004 *Phys. Rev. B* **70** 134102
[13] Arlt T, Bermejo M, Blanco M A, Gerward L, Jiang J Z, Staun Olsen J, Recio J M and Recio J M 2000 *Phys. Rev. B* **61** 14414
[14] Pischedda V, Hearne G R, Dawe A M and Lowther J E 2006 *Phys. Rev. Lett.* **96** 035509
[15] Swamy V, Kuznetsov A, Dubrovinsky L S, McMillan P F, Prakapenka V B, Shen G Y and Muddle B C 2006 *Phys. Rev. Lett.* **96** 135702
[16] Flank A M, Lagarde P, Itie J P, Polian A and Hearne G R 2008 *Phys. Rev. B* **77** 224112
[17] Park S, Jang J, Cheon J, Lee H H, Lee D R and Lee Y 2008 *J. Phys. Chem. C* **112** 9627
[18] Li Q J, Cheng B Y, Yang X, Liu R, Liu B, Liu J, Chen Z Q, Zou B, Cui T and Liu B B 2013 *J. Phys. Chem. C* **117** 8516
[19] Dong Z H and Song Y 2015 *Can. J. Chem.* **93** 165
[20] Li Q J, Cheng B Y, Tian B L, Liu R, Liu B, Wang F, Chen Z Q, Zou B, Cui T and Liu B B 2014 *RSC Adv.* **4** 12873
[21] Li Q J, Liu B B, Wang L, Li D M, Liu R, Zou B, Cui T, Zou G T, Meng Y, Mao H K, Liu Z X, Liu J and Li J X 2010 *J. Phys. Chem. Lett.* **1** 309
[22] Wang Z W, Saxena S K, Pischedda V, Liermann H P and Zha C S 2001 *J. Phys.: Condens. Matter* **13** 8317
[23] Gerward L and Olsen J S 1997 *J. Appl. Crystallogr.* **30** 259
[24] Jamieson J C and Olinger B 1968 *Science* **161** 893
[25] Sasaki T 2002 *J. Phys.: Condens. Matter* **14** 10557
[26] Montanari B and Harrison N M 2004 *J. Phys.: Condens. Matter* **16** 273
[27] Wu X, Holbig E and Steinle-Neumann G 2010 *J. Phys.: Condens. Matter* **22** 295501
[28] He Y, Liu J F, Chen W, Wang H, Zeng Y W, Zhang G Q, Wang L N, Liu J, Hu T D, Hahn H, Gleiter H and Jiang J Z 2005 *Phys. Rev. B* **72** 212102
[29] Wu H M, Wang Z W and Fan H Y 2014 *JACS* **136** 7634
[30] Quan Z W, Luo Z P, Wang Y X, Xu H W, Wang C Y, Wang Z W and Fang J Y 2013 *Nano Lett.* **13** 3729
[31] Swamy V, Dubrovinsky L S, Dubrovinskaia N A, Langenhorst F, Simionovici A S, Drakopoulos M, Dmitriev V and Weber H P 2003 *Solid State Commun.* **125** 111
[32] Al-Khatatbeh Y, Lee K K M and Kiefer B 2012 *J. Phys. Chem. C* **116** 21635
[33] Machon D, Daniel M, Bouvier P, Daniele S, Floch S L, Melinon P and Pischedda V 2011 *J. Phys. Chem. C* **115** 22286
[34] Mishima O, Calvert L D and Whalley E 1984 *Nature* **310** 393
[35] Deb S K, Wilding M, Somayazulu M and McMillan P F 2001 *Nature* **414** 528
[36] Hemley R J, Jephcoat A P, Mao H K, Ming L C and Manghnan M H 1988 *Nature* **334** 52
[37] Wang L, Yang W G, Ding Y, Ren Y, Xiao S G, Liu B B, Sinogeikin S V, Meng Y, Gosztola D J, Shen G R, Hemley R J, Mao W L and Mao H K 2010 *Phys. Rev. Lett.* **105** 095701
[38] Yang X, Li Q J, Liu Z D, Bai X, Song H W, Yao M G, Liu b, Liu R, Gong C, Lu S C, Yao Z, Li D M, Liu J, Chen Z Q, Zou B, Cui T and Liu B B 2013 *J. Phys. Chem. C* **117** 8503
[39] Hoang V V 2007 *J. Phys. D: Appl. Phys.* **40** 7454
[40] Machon D, Daniel M, Pischedda V, Daniele S, Bouvier P and LeFloch S 2010 *Phys. Rev. B* **82** 140102
[41] McMillan P F 2004 *J. Mater. Chem.* **14** 1506
[42] Mishima O, Calvert L D and Whalley E 1985 *Nature* **314** 76
[43] McMillan P F, Wilson M, Daisenberger D and Machon D 2005 *Nat. Mater.* **4** 680
[44] Li Q J, Liu R, Cheng B Y, Wang L, Yao M G and Li D M 2012 *Mater. Res. Bull.* **47** 1396
[45] Wang Y J, Zhang J Z, Wu J, Coffer J L, Lin Z J, Sinogeikin S V, Yang W G and Zhao Y S 2008 *Nano Lett.* **8** 2891
[46] Zardo I, Yazji S, Marini C, Uccelli E, Morral A F, Abstreiter G and Postorino P 2012 *ACS Nano* **6** 3284
[47] Lin Yu, Yang Y, Ma H W, Cui Y and Mao W L 2011 *J. Phys. Chem. C* **115** 9844
[48] Wang Z W, Daemen L L, Zhao Y S, Zha C S, Downs R T, Wang X D, Wang Z L and Hemley R 2005 *Nat. Mater.* **13** 1
[49] Wang L H, Liu H Z, Qian J, Yang W G and Zhao Y S 2012 *J. Phys. Chem. C* **116** 2074
[50] Li Q J, Liu R, Liu B B, Wang L, Wang K, Li D M, Zou B, Cui T, Liu J, Chen Z Q and Yang K 2012 *RSC Adv.* **2** 9052
[51] Olsen J S, Gerward L and Jiang J Z 2002 *High Pressure Res.* **22** 385